

# DUNI model and $H_0$ tensions

Mohammad Hadi Mohammadi<sup>1</sup>

email [hadi.symbol@gmail.com](mailto:hadi.symbol@gmail.com)

<sup>1</sup> *Department of Physics, Bu-Ali Sina University, Hamedan 65178, 016016, Iran*

In this study, we introduce the Dark Universe (DUNI) model, a novel cosmological framework addressing the Hubble tension and the fine-tuning problem associated with vacuum energy. Unlike the  $\Lambda$ CDM model, which exhibits significant discrepancies with the R21 (Adam Rises) data, the DUNI model proposes that dark energy, rather than radiation, dominates the early universe's expansion. This distinctive approach significantly reduces the Hubble tension to a consistency level of  $0.22\sigma$  while maintaining the same number of free parameters as the  $\Lambda$ CDM model. By assuming an exponential function for dark energy and its effects on matter, the DUNI model also addresses the hierarchy problem by predicting a lower effective mass for particles like the Higgs boson in the early universe. Using CosmoMC tools, we validate the DUNI model against observational datasets including R21(Adam Riess), Type Ia Pantheon supernovae, the cosmic microwave background (CMB), and baryon acoustic oscillations (BAO), demonstrating its robust compatibility with current observations.

## I. INTRODUCTION

The  $\Lambda$ CDM model has long served as the standard paradigm in cosmology, successfully describing the universe's large-scale structure and expansion history [1]. It integrates a cosmological constant ( $\Lambda$ ) as dark energy and cold dark matter (CDM) to account for the observed accelerated expansion and the formation of cosmic structures. However, the  $\Lambda$ CDM model faces significant challenges: the Hubble tension, a persistent discrepancy between locally measured and early universe-inferred expansion rates, and the fine-tuning problem regarding the disparity between predicted and observed vacuum energy densities [2].

Moreover, the  $\Lambda$ CDM model shows substantial discrepancies when fitted to the R21 (Adam Rises) data, highlighting its limitations in describing the universe's expansion history accurately [3]. In contrast, we propose the Dark Universe (DUNI) model, which posits that dark energy, rather than radiation, dominates the early expansion of the universe. This paradigm shift resolves the fine-tuning problem by aligning theoretical and observed vacuum energy densities more closely and provides better constraints on the R21 data, significantly reducing the Hubble tension to  $0.22\sigma$ .

Additionally, the DUNI model addresses the hierarchy problem by predicting that dark energy influences matter in a way that lowers the effective mass of particles like the Higgs boson in the early universe. This is achieved through the relationship  $H_{DE}(z) = H_0 e^{\frac{1}{2}z}$ , which we demonstrate solves the hierarchy problem around a redshift of 30, consistent with current observations [4].

This study evaluates the DUNI model at the background level, examining its fundamental cosmological dynamics and compatibility with observational data. Utilizing the CosmoMC computational framework, we integrate data from R21, Type Ia Pantheon supernovae, the CMB, and BAO to validate the DUNI model's consistency with observed phenomena.

## II. MODEL DESCRIPTION

The DUNI model proposes a novel framework in which dark energy plays a crucial role in the early universe's expansion, rather than radiation. The core of the model is based on the assumption that Hubble dark energy-dominated era can be described as  $H_{DE}(z) = H_0 e^{\frac{1}{2}z}$ . This relationship suggests that dark energy exponentially impacts the expansion rate and the matter energy density, leading to significant cosmological implications. The DUNI model proposes that dark energy, rather than radiation, dominates the early universe's expansion. This model assumes that the Hubble parameter,  $H(z)$ , evolves according to:

$$H = H_0 \sqrt{\Omega_{DE0} e^z + \Omega_{m0} e^{-2z} (1+z)^4 + \Omega_{r0} (1+z)^4} \quad (1)$$

Where  $\Omega_m = \Omega_{DM} + \Omega_b$  is the total mass density parameter including dark matter and baryonic matter and,  $\Omega_r$  is the density parameter of radiation (photons+relativistic neutrinos).

### A. Hubble Function for Dark Energy Density

To derive the Hubble function in the context of the DUNI model, we start with the differential equation governing dark energy:

$$\dot{\rho}_{DE} + 3H\rho_{DE}(1+w) = f(z) \quad (2)$$

Assuming  $\rho_{DE} = \frac{3H^2}{8\pi G}$ , we have:

$$\frac{6\dot{H}H}{8\pi G} + 3H\rho_{DE}(1+w) = f(z) \quad (3)$$

$$f(z) = S(z)H^2 \quad (4)$$

$$\frac{6}{8\pi G}H\frac{dH}{dt} + 3H\frac{3H^2}{8\pi G}(1+w) = S(z)H^2 \quad (5)$$

Dividing by  $H^2$  and integrating, we get:

$$\frac{6}{8\pi G}\frac{dH}{H} + 3H\frac{3}{8\pi G}(1+w)dt = S(z)dt \quad (6)$$

Using  $H = \frac{da}{dt}\frac{1}{a} \rightarrow dt = \frac{da}{aH}$

$$\frac{6}{8\pi G}\frac{dH}{H} + \frac{9}{8\pi G}(1+w)\frac{da}{a} = S(z)dt \quad (7)$$

Finally, integrating yields:

$$H(z) = H_0 e^{\int (\frac{8\pi G}{6}S(z)dt - \frac{3}{2}(1+w)\frac{da}{a})} = H_0 e^{X(z)} \quad (8)$$

where we define  $X(z) = \frac{1}{2}z$  to align with the exponential dark energy function  $H_{DE}(z) = H_0 e^{\frac{1}{2}z}$

### B. Matter Density Relation

While we cannot theoretically prove the exact form of the matter density relation, we can test its validity through observational consistency. For  $w=0$ , the Hubble function is given by:

$$\begin{aligned} \dot{\rho}_m + 3H\rho_m(1+w) &= g(z) \\ w &= 0 \\ g(z) &= N(z)H^2(z) \\ H(z) &= H_0 e^{\int (\frac{8\pi G}{6}N(z)dt - \frac{3}{2}\frac{da}{a})} = H_0 e^{\int (\frac{8\pi G}{6}N(z)dt + \frac{3}{2}\frac{dz}{1+z})} = H_0(1+z)^{\frac{3}{2}}e^{V(z)} \end{aligned} \quad (9)$$

Assuming that dark energy affects matter, we propose:

$$e^{V(z)} = \frac{M(z)}{E_{DE}^2(z)} \quad (10)$$

Guessing  $M(z) = (1+z)^{\frac{1}{2}}$ , we obtain:

$$e^{V(z)} = \frac{(1+z)^{\frac{1}{2}}}{\frac{H_{DE}^2(z)}{H_0^2}} = e^{-z}(1+z)^{\frac{1}{2}} \quad (11)$$

Thus,

$$\begin{aligned} H(z) &= H_0(1+z)^{\frac{3}{2}}e^{V(z)} = H_0(1+z)^{\frac{3}{2}}(1+z)^{\frac{1}{2}}e^{-z} \\ H(z) &= H_0e^{-z}(1+z)^2 \end{aligned} \quad (12)$$

Hence, the matter density relation becomes:

$$\rho_m = \frac{3H^2}{8\pi G} \quad (13)$$

$$\rho_m = \frac{3H_0^2}{8\pi G} \frac{(1+z)}{\left(\frac{H_{DE}^2(z)}{H_0^2}\right)^2} (1+z)^3 = \frac{3H_0^2}{8\pi G} \frac{1}{E_{DE}^4(z)} (1+z)^4 \quad (14)$$

$$\rho_m = \frac{3H_0^2}{8\pi G} e^{-2z} (1+z)^4 \quad (15)$$

We assume a matter density relation and find it compatible with observations by substituting it into the DUNI model and checking its predictions. This empirical approach shows that the assumed matter density relation provides a good fit to the data, reinforcing its validity within the model's framework.

### C. Estimating Redshift for Boson Generation and Addressing the Hierarchy Problem

The hierarchy problem concerns the vast difference between the Higgs boson's observed mass and the large quantum corrections it should receive from high-energy processes. In the DUNI model, this problem is mitigated by the influence of dark energy on matter properties. The energy density of dark energy at high redshifts affects the mass of particles like the Higgs boson, resulting in lower effective masses in the early universe.

### D. Redshift Estimation

To estimate the redshift  $z$  at which the hierarchy problem is addressed and bosons like the Higgs are generated, we use the matter density relation derived above. For  $z \approx 30$  so we have:

$$\begin{aligned} \rho_{Higgs} &\approx \frac{3H_0^2}{8\pi G} e^{-2z} (1+z)^4 \\ Atz &\approx 30 \\ \rho_{Higgs} &\approx \frac{3H_0^2}{8\pi G} e^{-60} (31)^4 \end{aligned} \quad (16)$$

This high redshift corresponds to a significantly reduced energy density, consistent with conditions required for particle generation in the early universe. Observations suggest that such redshifts are indeed where significant structure formation and particle generation occur.

### E. Solution of Fine-Tuning Problem

The fine-tuning problem in cosmology concerns the discrepancy between the theoretical prediction and the observed value of vacuum energy. In the DUNI model, the vacuum energy density at high redshift can be expressed as

$$\rho_{vacuum} = \frac{3H_0^2}{8\pi G} (\Omega_{DE0} e^z + \Omega_{m0} e^{-2z} (1+z)^4 + \Omega_{r0} (1+z)^4) \quad (17)$$

At high redshifts, where  $z$  is large the term  $\Omega_{DE0} e^z$  dominates, and we have:

$$\rho_{vacuum}(z \gg 1) \approx \frac{3H_0^2 \Omega_{DE0}}{8\pi G} e^z \quad (18)$$

This exponential term aligns the theoretical prediction with the observed vacuum energy density by adjusting the value of  $\Omega_{DE0}$  to match observations. This effectively resolves the fine-tuning problem by ensuring that the predicted vacuum energy density does not vastly exceed the observed value. The DUNI model derives its predictions from General Relativity (GR) while aligning with Quantum Field Theory (QFT) predictions for vacuum energy, providing a unified approach to these fundamental problems.

### III. IMPORTANT NOTE ABOUT RECENT SUPERNOVA DATA (ADAM RIESS 2021)(R21)

His data set, potentially involving Type Ia supernovae, offers valuable insights into the universe’s expansion history at higher redshifts. The DUNI model can be compared to this recent data (2021) from Adam Riess and collaborators to assess its ability to reconcile the Hubble tension, particularly if it provides a better fit with the observed  $H_0$  value compared to the Lambda-CDM model.

By incorporating these diverse data sets at the background level into its analysis using the Cosmo MC computational tool, the DUNI model can be rigorously tested against observations. A better fit with these data sets, including the recent supernova data from Adam Riess et al. (2021), could potentially contribute to resolving the Hubble tension.

### IV. OBSERVATIONAL DATA

In this section, we describe the cosmological data sets used in this work in brief. The description of the data catalogs is as follows:

1. **CMB**: We use the most precise full-sky measurements of Cosmic Microwave Background (CMB) radiation performed by *Planck* satellite. We use both high- $\ell$  temperature and polarization angular power spectra from the final release of “*Planck 2018*” baseline PLIK-TTTEEE along with *Planck* low- $\ell$  and low-E (SimAll) ( $\ell \leq 30$ ) [5–7]. We mention all of *Planck* data (including temperature and polarization) by “CMB”.
2. **R21**: To test the ability of this model to reconcile the  $H_0$  tension, we additionally include a Gaussian prior of the form  $H_0 = 73.30 \pm 1.04$  km/s Mpc, as reported by the SH0ES Collaboration [3]. We refer to this prior as “R21”.
3. **BAO**: We also consider the various measurements of the Baryon Acoustic Oscillations (BAO) from different galaxy surveys as the *Planck* collaboration in their 2018 analysis [5], i.e. 6dFGS [8], SDSS-MGS [9], and BOSS DR12 [10]. We mention all these data points by “BAO”.
4. **SN**: We include the measurements of the 1048 Supernovae Type Ia luminosity distance in the red-shift interval  $z \in [0.01, 2.3]$ , from the Pantheon sample [11]. We show this catalog of SuperNovae by “SN”.

In some analysis, we use a combination of “CMB+BAO+SN” data which we refer to this combination as “CBS”.

### V. STATISTICAL METHODS

Here, we briefly introduce the statistical methods used in our analysis. The cosmological analysis we carry out in this work is based on Bayesian inference. To analyze the data and extract the constraints on the cosmological parameters for DUNI model, we have modified carefully the widely used cosmological Markov Chain Monte Carlo package *CosmoMC* [12, 13], which is publicly available[<http://cosmologist.info/cosmomc>]. This package is equipped with a convergence diagnostic based on the Gelman and Rubin statistic [14], assuming  $|R - 1| < 0.01$  for all parameters, and implements an efficient sampling of the posterior distribution using the fast/slow parameter decorrelations [13].

One measure to check the consistency of our model with observational data in comparison to the standard model is the “Akaike Information Criterium” (AIC) which is a tool to measure the improvement of the fit. We compute the AIC of the extended model DUNI relative to that of  $\Lambda$ CDM, defined as

$$\Delta\text{AIC} = \chi_{\min, \text{DUNI}}^2 - \chi_{\min, \Lambda\text{CDM}}^2 + 2(N_{\text{DUNI}} - N_{\Lambda\text{CDM}}), \quad (19)$$

where  $N_{\text{DUNI}}$  and  $N_{\Lambda\text{CDM}}$  stand for the number of free parameters of DUNI model and  $\Lambda$ CDM model [15, 16], respectively.

To put the model to the test for Hubble tension we use the “rule of thumb difference in mean” or Gaussian Tension (GT) [16, 17], defined as

$$\frac{\bar{x}_{\mathcal{D}} - \bar{x}_{\text{SH0ES}}}{(\sigma_{\mathcal{D}}^2 + \sigma_{\text{SH0ES}}^2)^{1/2}}, \quad (20)$$

where  $\bar{x}_{\mathcal{D}}$  and  $\sigma_{\mathcal{D}}$  are the mean and standard deviation of the  $H_0$  for model based on observational data  $\mathcal{D}$ , and  $\bar{x}_{\text{SH0ES}}$  and  $\sigma_{\text{SH0ES}}$  correspond to  $H_0 = 73.30 \pm 1.04$  km/s Mpc [3].

We do a Maximum Likelihood Analysis by using `CosmoMC` as a cosmological MCMC code. To find the best fit of parameters of DUNI model, we assume a parameter space as:

$$\mathcal{P}_0 \equiv \left\{ \Omega_b h^2, \Omega_c h^2, 100\theta_{\text{MC}}, \tau, \ln[10^{10} A_s], n_s \right\}, \quad (21)$$

where  $\tau_{\text{re}}$  is the reionization optical depth,  $n_s$  is the scalar spectral index,  $A_s$  is the amplitude of the scalar primordial power spectrum, and  $\Theta_{\text{MC}}$  is an approximation of  $\theta_*$ , which represents the angular scale of the sound horizon at decoupling. We always consider a flat Universe ( $\Omega_K = 0$ ). The priors assumed for parameters are summarized in Table I.

To do cosmological calculation for DUNI model, we used a publicly available Einstein-Boltzmann code, called `CAMB` code [18]. By careful modification of `CAMB` code for this model, we obtained power spectrum of temperature anisotropies (see Fig. 8).

## VI. RESULTS

To put our model to the test, we applied many combination of observational data including Early-universe data (CMB), Standard Rulers (BAO), Standard Candles (SuperNovae) and also a prior of  $H_0$  parameter extracted by SH0ES team [3]. As, we can see in Fig. 1, the prediction of our model for  $H_0$  parameter is pretty consistent with late-time measurement of Hubble parameter called ‘‘R21’’ [3]. In this figure, the shaded area represents the measurement of  $H_0$  parameter according to SH0ES team. The result of analysis of model based on only CMB data (Temperature and Polarization together) shows fully consistency with ‘‘R21’’ measurement. Similar conclusion can be inferred from Fig. 2. The two-dimensional contour plots of  $H_0$  parameter vs. density parameter of matter  $\Omega_m$  show that by applying different data combination including: CMB, CMB+SN, CMB+R21 and CMB+SN+R21 to our model, it shows consistency with ‘‘R21’’ measurement completely. But, similar to  $\Lambda$ CDM model, when we add Baryon Acoustic Oscillation (BAO) data, it goes away. However, we should note that in our model in contrast to  $\Lambda$ CDM model, the contour of ‘‘CMB+BAO+SN’’ analysis shows overlap with ‘‘R21’’ measurement and it is not fully incompatible with late-time measurement of  $H_0$  parameter.

In Fig. 3 we show the one-dimensional posterior of different parameters when we apply different combination of data to our model. Also, similar result for different parameters is depicted in Fig. 4.

In Table. II we see result of analysis for  $\Lambda$ CDM model with different combination of data. And, in Table. III we summarize the result of analysis of our model with different data combination. According to these tables, by using the definition of Gaussian Tension in Eq. 20 our model has the ability to reduce the tension in Hubble parameter to  $0.22\sigma$ . Please note that this accomplishment while it is obtained that the number of free parameters of our model is similar to Standard model.

The visual result comparing  $\Lambda$ CDM model and DUNI model by using only CMB data can be seen in Fig. 6. The visual result for DUNI model by using only CMB data can be seen in Fig. 5. The vertical and horizontal dashed lines show best-fit value of ‘‘R21’’ measurement for  $H_0$  parameter. Obviously our model fit within ‘‘R21’’ constraint very well while  $\Lambda$ CDM shows significant discrepancy.

For more intuition, we show the summarized result of Table. III in graphical way in Fig. 7. We can see behavior of model parameters when we apply different data combination.

The most important statistical property of CMB anisotropies is the ‘‘power spectrum’’. We compare power spectrum of DUNI model with  $\Lambda$ CDM and observational data points of *Planck 2018* data release in Fig. 8. The shaded area, represents the limit for accuracy of the power spectrum called ‘‘Cosmic Variance’’ which is defined as [19]

$$\left( \frac{\Delta C(\ell)}{C(\ell)} \right)_{\text{cosmicvariance}} = \sqrt{\frac{2}{2\ell + 1}} \quad (22)$$

Where  $\ell$  is the multipole moment and  $C(\ell)$  is the power spectrum.

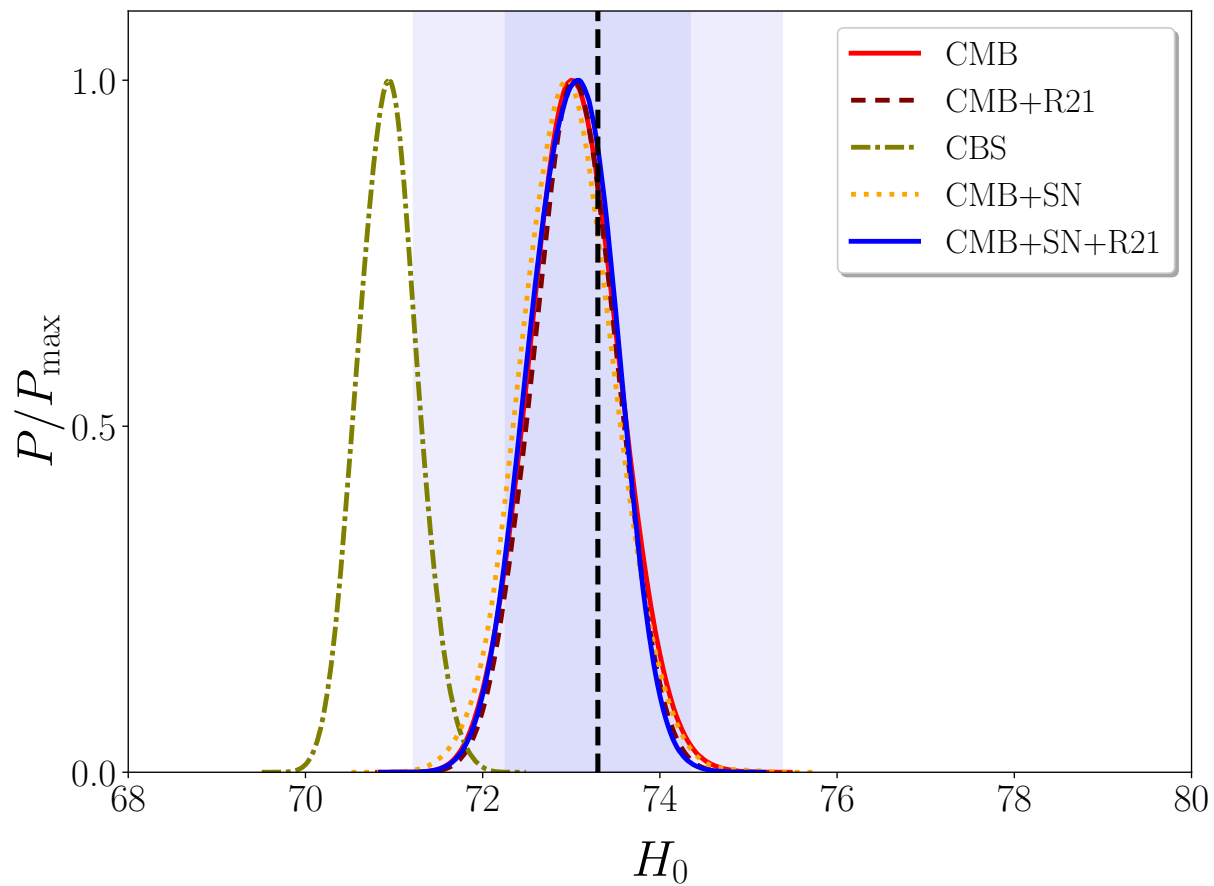


FIG. 1. 1D posteriors of  $H_0$  are shown for the different dataset combinations. The shaded area shows the measurement of  $H_0$  done by the SH0ES team and its  $1\sigma$  and  $2\sigma$  errors [3].

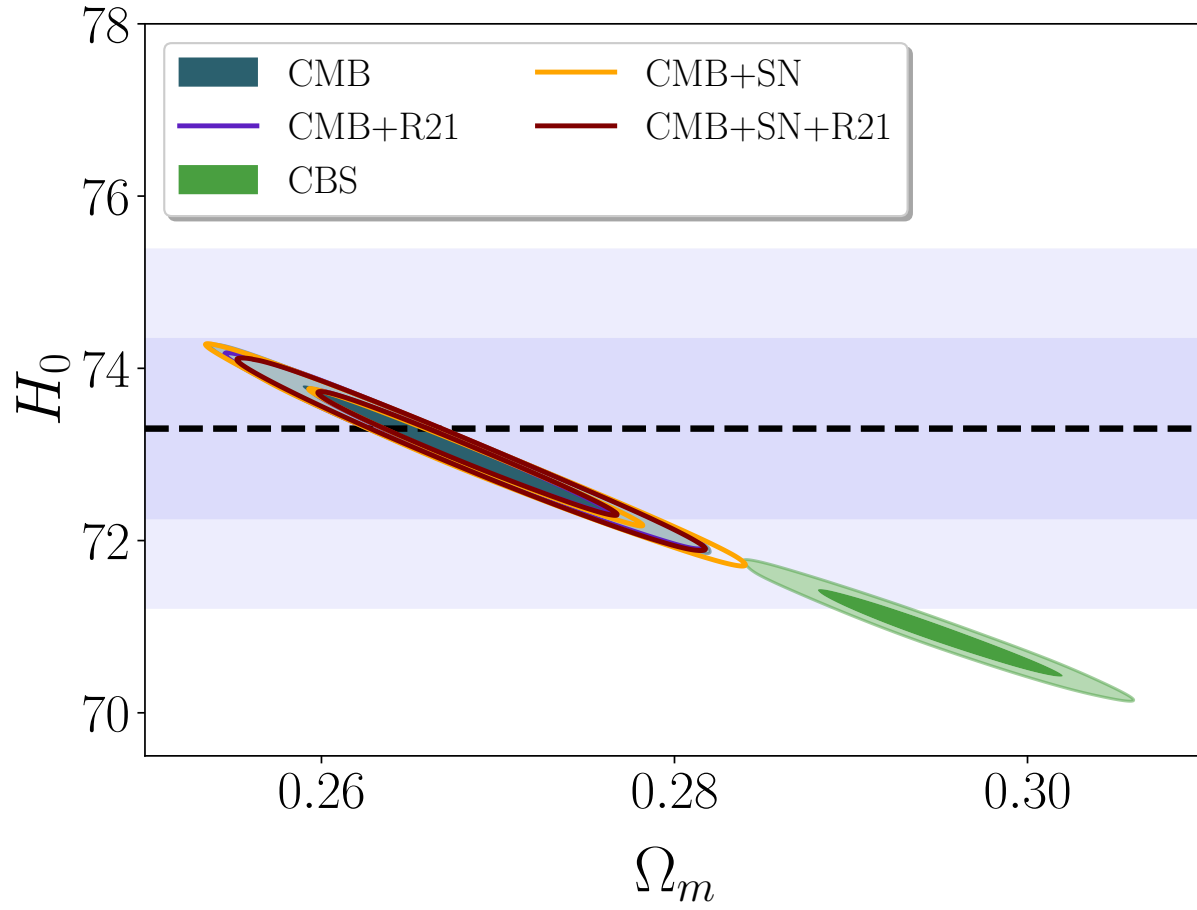


FIG. 2. 2D contour plots at  $1\sigma$  and  $2\sigma$  confidence levels for  $H_0$  vs.  $\Omega_m$  for the DUNI model for different combination of data. The dashed line marker is a central value of the  $H_0$  measurement reported by the SH0ES team (R21) and the shaded area shows the  $1\sigma$  and  $2\sigma$  confidence levels of this measurement.

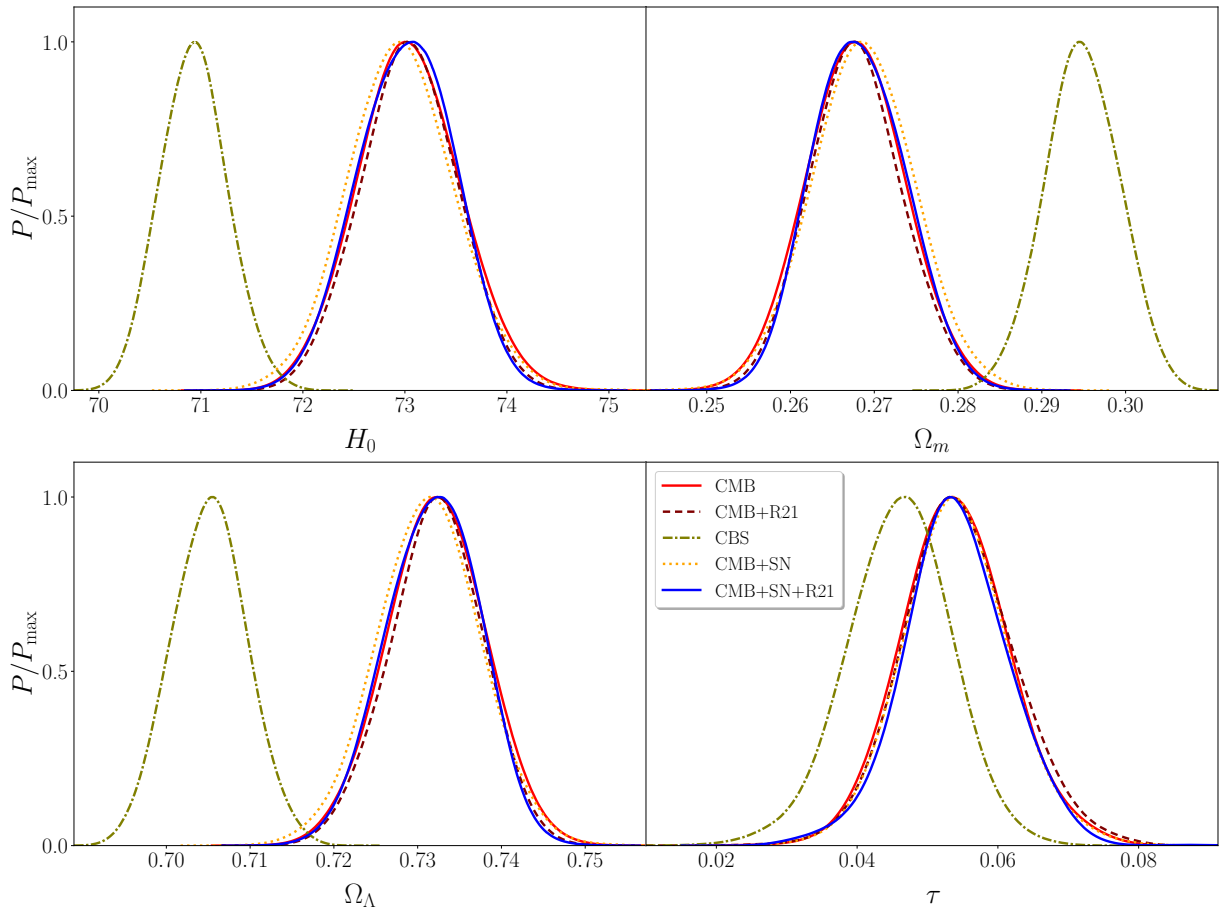


FIG. 3. 1D posteriors of different parameters are shown for the different dataset combinations.



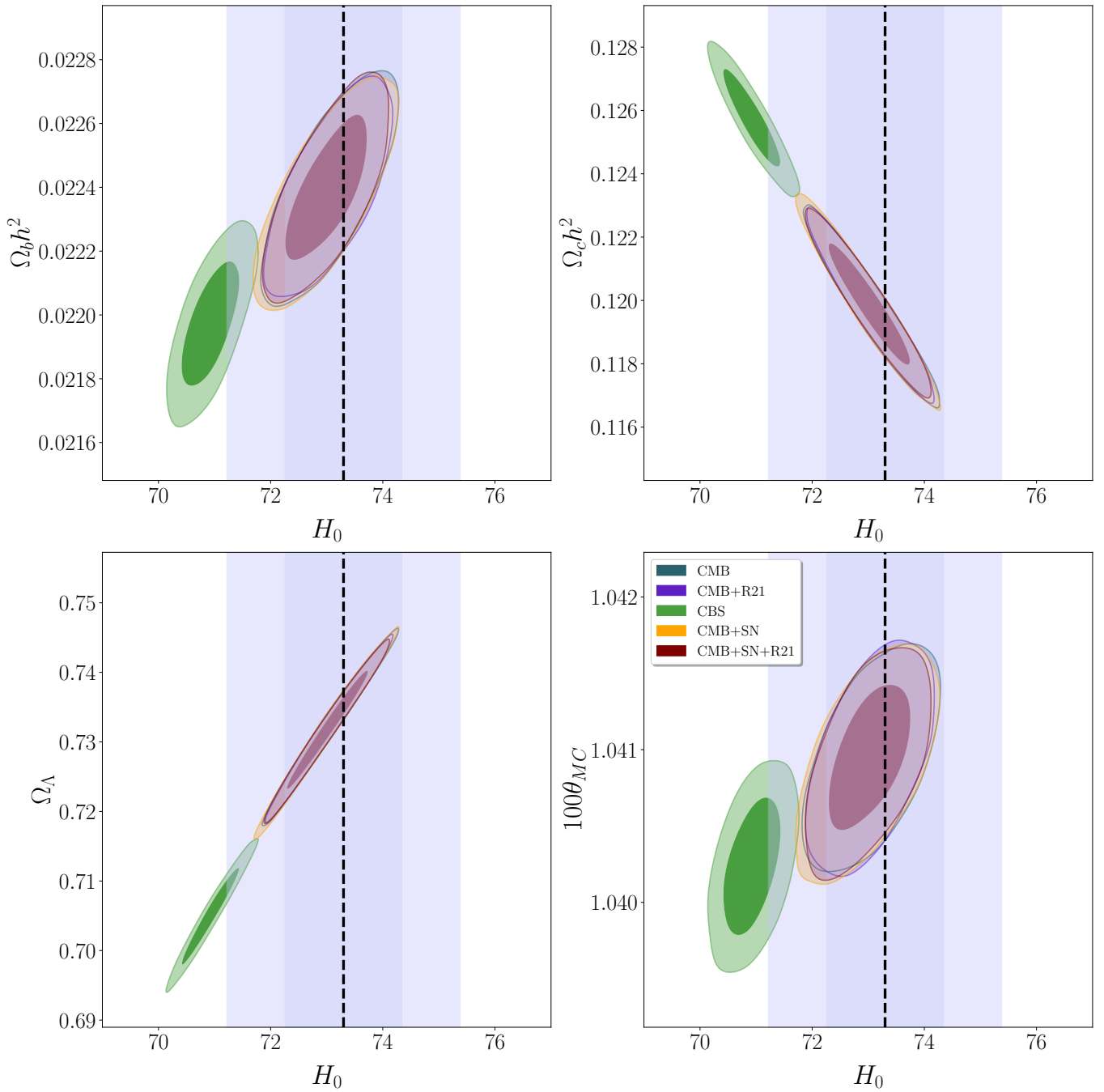


FIG. 4. 2D contour plots of  $H_0$  vs. the parameters  $\epsilon$ ,  $\ln[10^{10} A_s]$ , and Tensor-to-Scalar ratio  $r$  for the DUNI model for different combination of data. The vertical dashed line in the upper panel indicates the measurement of the Hubble parameter made by [3] and the shaded area depicts the  $1\sigma$  and  $2\sigma$  error bars.

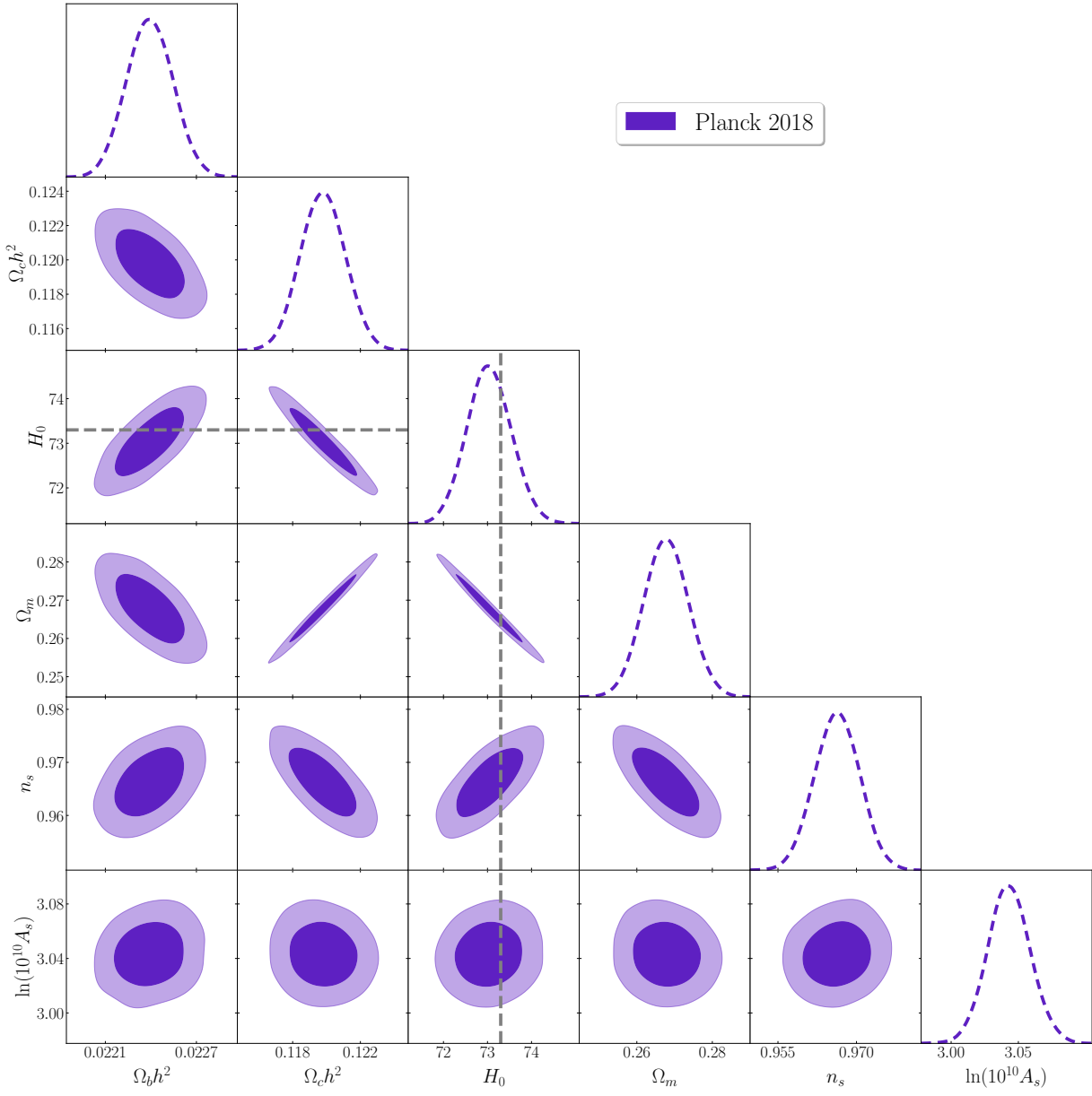


FIG. 5. Contours and likelihoods of different parameters of DUNI model based on only *Planck 2018* temperature and polarization data.

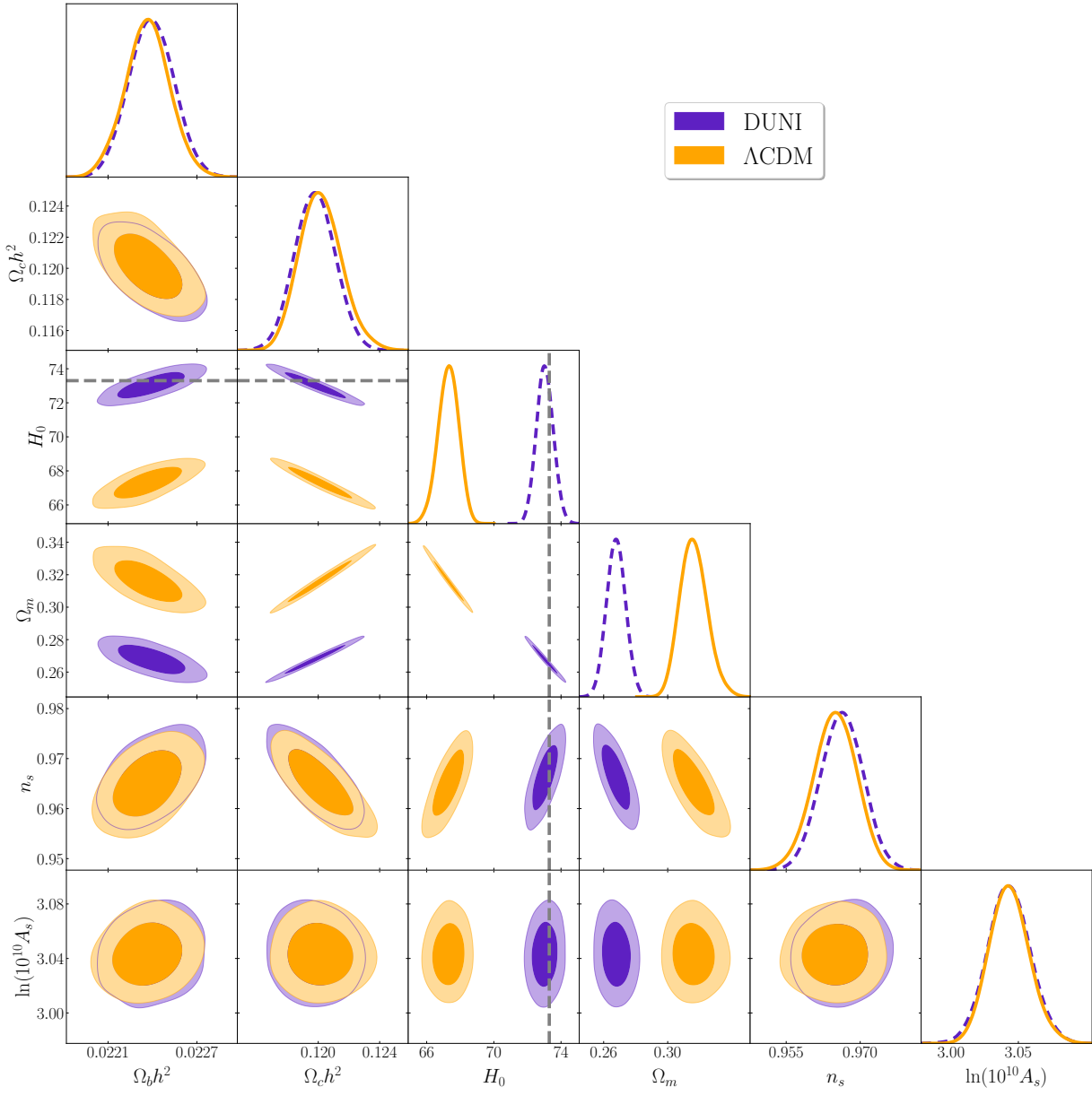


FIG. 6. Comparison between DUNI model and  $\Lambda$ CDM model based on *Planck 2018* temperature and polarization data.

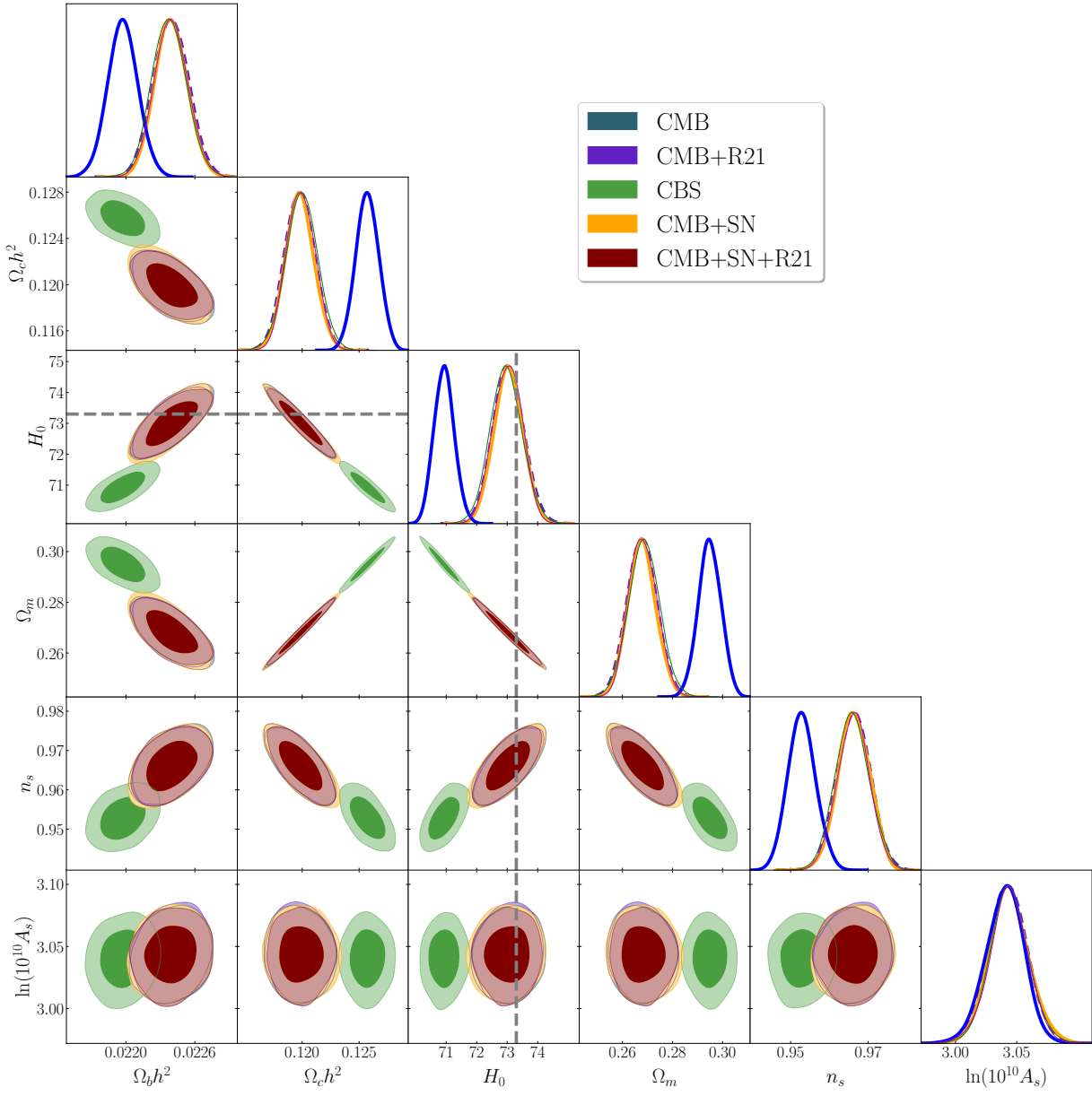


FIG. 7. DUNI model based on *Planck 2018* temperature and polarization data.

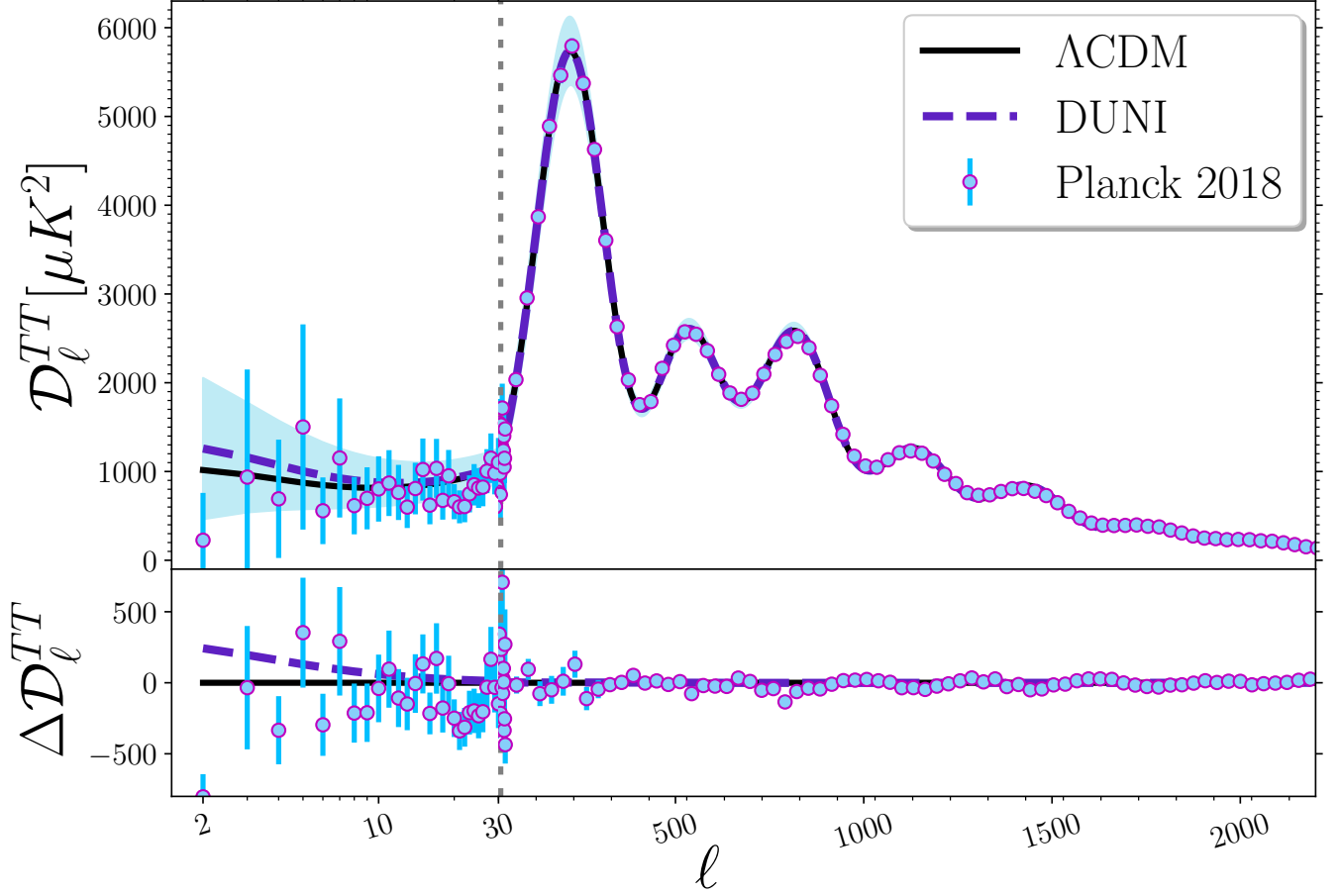


FIG. 8. Power spectrum of the temperature anisotropies for the DUNI model with a dashed orange line obtained with the best-fit of the parameters for the “CMB”. The theoretical prediction of the  $\Lambda$ CDM model is shown with a solid black line. Blue points show observational data of *Planck* 2018 release. The shaded area represents the cosmic variance of the power spectrum. The lower panel shows the residual of the two models to observational data.

Parameter	Priors
$\Omega_b h^2$	[0.005, 0.1]
$\Omega_c h^2$	[0.001, 0.99]
$\tau_{\text{re}}$	[0.01, 0.8]
$100\Theta_{\text{MC}}$	[0.5, 10]
$\log [10^{10} A_s]$	[1.6, 3.91]
$n_s$	[0.8, 1.2]

TABLE I. Flat priors used on various free parameters of DUNI model, during statistical analysis.

Parameter	CMB	CMB+R21	CBS	CMB+SN	CMB+SN+R21
$\Omega_m$	$0.3162^{+0.0078}_{-0.0091}$	$0.2958 \pm 0.0068$	$0.3100 \pm 0.0060$	$0.3148 \pm 0.0080$	$0.2959 \pm 0.0065$
$H_0$	$67.30 \pm 0.61$	$68.84 \pm 0.53$	$67.74 \pm 0.44$	$67.40 \pm 0.58$	$68.83 \pm 0.51$
$\tau$	$0.0537 \pm 0.0073$	$0.0595^{+0.0072}_{-0.0086}$	$0.0558 \pm 0.0079$	$0.0548 \pm 0.0080$	$0.0540 \pm 0.0076$
$100\theta_{MC}$	$1.04090 \pm 0.00031$	$1.04133 \pm 0.00029$	$1.04102 \pm 0.00030$	$1.04093 \pm 0.00031$	$1.04133 \pm 0.00030$
$n_s$	$0.9649 \pm 0.0043$	$0.9729 \pm 0.0041$	$0.9673 \pm 0.0038$	$0.9654 \pm 0.0044$	$0.9662 \pm 0.0041$
$\ln(10^{10} A_s)$	$3.043 \pm 0.015$	$3.048^{+0.015}_{-0.018}$	$3.046 \pm 0.016$	$3.045 \pm 0.016$	$3.048 \pm 0.017$
$\chi^2_{R21}$	---	18.7 ( $\nu$ : 9.8)	---	---	18.7 ( $\nu$ : 8.9)
$\chi^2_{BAO}$	---	---	6.0 ( $\nu$ : 0.5)	---	---
$\chi^2_{SN}$	---	---	1035.06 ( $\nu$ : 0.0)	1035.37 ( $\nu$ : 0.2)	1034.84 ( $\nu$ : 0.0)
$\chi^2_{CMB}$	2780.0 ( $\nu$ : 15.0)	2786.3 ( $\nu$ : 26.6)	2780.4 ( $\nu$ : 16.9)	2780.1 ( $\nu$ : 16.8)	2786.4 ( $\nu$ : 25.2)
$\Delta AIC$	0	0	0	0	0

TABLE II. 68 % CL constraints on free and derived parameters of the  $\Lambda$ CDM model from *Planck* CMB power spectra in combination with BAO and Type Ia SuperNovae data plus a Gaussian prior on the Hubble constant  $H_0$  as measured by SHOES team.

Parameter	CMB	CMB+R21	CBS	CMB+SN	CMB+SN+R21
$\Omega_m$	$0.2678 \pm 0.0059$	$0.2678 \pm 0.0055$	$0.2949 \pm 0.0045$	$0.2686 \pm 0.0062$	$0.2681 \pm 0.0056$
$H_0$	$73.04 \pm 0.50$	$73.04 \pm 0.47$	$70.93 \pm 0.33$	$72.97 \pm 0.52$	$73.02 \pm 0.47$
$\tau$	$0.0539 \pm 0.0078$	$0.0545 \pm 0.0081$	$0.0459 \pm 0.0075$	$0.0541 \pm 0.0077$	$0.0540 \pm 0.0076$
$100\theta_{MC}$	$1.04094 \pm 0.00031$	$1.04095 \pm 0.00031$	$1.04024 \pm 0.00029$	$1.04092 \pm 0.00032$	$1.04095^{+0.00033}_{-0.00030}$
$n_s$	$0.9663 \pm 0.0043$	$0.9663 \pm 0.0041$	$0.9529 \pm 0.0036$	$0.9660 \pm 0.0044$	$0.9662 \pm 0.0041$
$\ln(10^{10} A_s)$	$3.043 \pm 0.016$	$3.044 \pm 0.016$	$3.040^{+0.016}_{-0.014}$	$3.044 \pm 0.016$	$3.043 \pm 0.016$
$\chi^2_{R21}$	---	0.27 ( $\nu$ : 0.1)	---	---	0.28 ( $\nu$ : 0.1)
$\chi^2_{BAO}$	---	---	32 ( $\nu$ : 18.2)	---	---
$\chi^2_{SN}$	---	---	1039.42 ( $\nu$ : 0.0)	1040.25 ( $\nu$ : 0.0)	1040.27 ( $\nu$ : 0.0)
$\chi^2_{CMB}$	2782.2 ( $\nu$ : 16.6)	2782.2 ( $\nu$ : 16.8)	2800.5 ( $\nu$ : 34.1)	2782.3 ( $\nu$ : 17.1)	2782.1 ( $\nu$ : 15.8)
$\Delta AIC$	2.2	-22.53	50.46	7.08	-17.29

TABLE III. 68 % CL constraints on free and derived parameters of the DUNI model from *Planck* CMB power spectra in combination with BAO and Type Ia SuperNovae data plus a Gaussian prior on the Hubble constant  $H_0$  as measured by SHOES team.

## VII. CONCLUDING REMARKS

The Dark Universe (DUNI) model offers a promising resolution to critical cosmological issues: the Hubble tension, the fine-tuning problem of vacuum energy, and the hierarchy problem. By proposing that dark energy dominates the early universe's expansion and assuming its exponential effect on matter, the DUNI model naturally aligns theoretical and observed vacuum energy densities. It significantly reduces the Hubble tension to  $0.22\sigma$ , particularly providing better constraints on the R21 (Adam Riess) data compared to the  $\Lambda$ CDM model.

Our analysis, focused on background-level dynamics, shows that the DUNI model aligns well with current observational data, maintaining the same number of free parameters as the  $\Lambda$ CDM model while providing a robust alternative for cosmic evolution. The compatibility of this energy density relation with observational data is further validated by the fact that it predicts a redshift of around 30 for the generation of the Higgs boson, consistent with current observations of the early universe.

The DUNI model thus emerges as a robust and viable alternative to  $\Lambda$ CDM, offering new insights into the universe's expansion history and fundamental properties.

## VIII. DATA AVAILABILITY STATEMENT

The datasets used or analysed during the current study available from the corresponding author on reasonable request.

## IX. CODE AVAILABILITY STATEMENT

The code used or analysed during the current study available from the corresponding author on reasonable request.

- 
- [1] S. Weinberg, The Cosmological Constant Problem, *Rev. Mod. Phys.* **61**, 1 (1989).
- [2] E. J. COPELAND, M. SAMI, and S. TSUJIKAWA, Dynamics of dark energy, *International Journal of Modern Physics D* **15**, 1753 (2006).
- [3] A. G. Riess *et al.*, A Comprehensive Measurement of the Local Value of the Hubble Constant with 1 km s<sup>-1</sup> Mpc<sup>-1</sup> Uncertainty from the Hubble Space Telescope and the SH0ES Team, *Astrophys. J. Lett.* **934**, L7 (2022), [arXiv:2112.04510 \[astro-ph.CO\]](#).
- [4] E. W. Kolb, *The Early Universe*, Vol. 69 (Taylor and Francis, 2019).
- [5] N. Aghanim *et al.* (Planck), Planck 2018 results. VI. Cosmological parameters, *Astron. Astrophys.* **641**, A6 (2020), [Erratum: *Astron. Astrophys.* 652, C4 (2021)], [arXiv:1807.06209 \[astro-ph.CO\]](#).
- [6] N. Aghanim *et al.* (Planck), Planck 2018 results. VIII. Gravitational lensing, *Astron. Astrophys.* **641**, A8 (2020), [arXiv:1807.06210 \[astro-ph.CO\]](#).
- [7] N. Aghanim *et al.* (Planck), Planck 2018 results. V. CMB power spectra and likelihoods, *Astron. Astrophys.* **641**, A5 (2020), [arXiv:1907.12875 \[astro-ph.CO\]](#).
- [8] F. Beutler, C. Blake, M. Colless, D. H. Jones, L. Staveley-Smith, L. Campbell, Q. Parker, W. Saunders, and F. Watson, The 6dF Galaxy Survey: Baryon Acoustic Oscillations and the Local Hubble Constant, *Mon. Not. Roy. Astron. Soc.* **416**, 3017 (2011), [arXiv:1106.3366 \[astro-ph.CO\]](#).
- [9] A. J. Ross, L. Samushia, C. Howlett, W. J. Percival, A. Burden, and M. Manera, The clustering of the SDSS DR7 main Galaxy sample – I. A 4 per cent distance measure at  $z = 0.15$ , *Mon. Not. Roy. Astron. Soc.* **449**, 835 (2015), [arXiv:1409.3242 \[astro-ph.CO\]](#).
- [10] S. Alam *et al.* (BOSS), The clustering of galaxies in the completed SDSS-III Baryon Oscillation Spectroscopic Survey: cosmological analysis of the DR12 galaxy sample, *Mon. Not. Roy. Astron. Soc.* **470**, 2617 (2017), [arXiv:1607.03155 \[astro-ph.CO\]](#).
- [11] D. M. Scolnic *et al.* (Pan-STARRS1), The Complete Light-curve Sample of Spectroscopically Confirmed SNe Ia from Pan-STARRS1 and Cosmological Constraints from the Combined Pantheon Sample, *Astrophys. J.* **859**, 101 (2018), [arXiv:1710.00845 \[astro-ph.CO\]](#).
- [12] A. Lewis and S. Bridle, Cosmological parameters from CMB and other data: A Monte Carlo approach, *Phys. Rev. D* **66**, 103511 (2002), [arXiv:astro-ph/0205436](#).
- [13] A. Lewis, Efficient sampling of fast and slow cosmological parameters, *Phys. Rev. D* **87**, 103529 (2013), [arXiv:1304.4473 \[astro-ph.CO\]](#).
- [14] A. Gelman and D. B. Rubin, Inference from Iterative Simulation Using Multiple Sequences, *Statist. Sci.* **7**, 457 (1992).
- [15] H. Akaike, A New Look at the Statistical Model Identification, *IEEE Transactions on Automatic Control* **19**, 716 (1974).
- [16] N. Schöneberg, G. Franco Abellán, A. Pérez Sánchez, S. J. Witte, V. Poulin, and J. Lesgourgues, The H0 Olympics: A fair ranking of proposed models, *Phys. Rept.* **984**, 1 (2022), [arXiv:2107.10291 \[astro-ph.CO\]](#).
- [17] M. Raveri and W. Hu, Concordance and Discordance in Cosmology, *Phys. Rev. D* **99**, 043506 (2019), [arXiv:1806.04649 \[astro-ph.CO\]](#).
- [18] A. Lewis, A. Challinor, and A. Lasenby, Efficient computation of CMB anisotropies in closed FRW models, *Astrophys. J.* **538**, 473 (2000), [arXiv:astro-ph/9911177](#).
- [19] S. Dodelson and F. Schmidt, *Modern Cosmology* (Elsevier Science, 2020).